

## Supporting Information

# A Hydrazone-based Covalent Organic Framework for Photocatalytic Hydrogen Evolution

Linus Stegbauer, Katharina Schwinghammer and  
Bettina V. Lotsch\*

*Max Planck Institute for Solid State Research Heisenbergstr. 1, 70569 Stuttgart, Germany*  
*Department of Chemistry, University of Munich (LMU), Butenandtstr. 5-13, 81377 München, Germany*  
*Nanosystems Initiative Munich (NIM) & Center for Nanoscience, Schellingstr. 4, 80799 München, Germany*

<b>A.</b>	<b>Materials and Instruments</b> .....	2
<b>B.</b>	<b>Synthetic Procedures</b> .....	3
<b>C.</b>	<b>FT-IR Spectra</b> .....	7
<b>D.</b>	<b>CP-MAS NMR Measurements</b> .....	8
<b>E.</b>	<b>Powder X-Ray Diffraction Data and Structure Simulation</b> .....	8
<b>F.</b>	<b>Sorption Measurements and Pore Size Distribution</b> .....	13
<b>G.</b>	<b>Plot of the Kubelka-Munk Function</b> .....	14
<b>H.</b>	<b>Stability of TFPT-COF in Organic Solvents and Water</b> .....	14
<b>I.</b>	<b>Reconversion of TFPT-COF after photocatalysis</b> .....	15
<b>J.</b>	<b>Photocatalysis</b> .....	19
<b>K.</b>	<b>Stability of TFPT-COF during photocatalysis</b> .....	20
<b>L.</b>	<b>References</b> .....	21

## A. Materials and Instruments

All reagents were purchased from commercial sources and used without further purification. The starter 2,5-diethoxy-terephthalohydrazide<sup>S1</sup> was prepared according to ref. S1, the NMR data being consistent with those given in the literature.

The synthesis of the second starting material TFPT<sup>S2</sup> is described below.

Infrared spectra were recorded on a Perkin Elmer Spektrum BX II FT-IR equipped with an ATR unit (Smith Detection Dura-Sample IIR diamond). The spectra were background-corrected.

The <sup>13</sup>C and <sup>15</sup>N MAS NMR spectra were recorded at ambient temperature on a Bruker Avance 500 solid-state NMR spectrometer, operating at frequencies of 500.1 MHz, 125.7 MHz and 50.7 MHz for <sup>1</sup>H, <sup>13</sup>C and <sup>15</sup>N, respectively. The sample was contained in a 4 mm ZrO<sub>2</sub> rotor (Bruker) which was mounted in a standard double resonance MAS probe. The <sup>13</sup>C and <sup>15</sup>N chemical shifts were referenced relative to TMS and nitromethane, respectively.

The <sup>1</sup>H-<sup>15</sup>N and <sup>1</sup>H-<sup>13</sup>C cross-polarization (CP) MAS spectra were recorded at a spinning speed of 10 kHz using a ramped-amplitude (RAMP) CP pulse on <sup>1</sup>H, centered on the *n* = +1 Hartmann-Hahn condition, with a nutation frequency  $\nu_{\text{nut}}$  of 55 kHz (<sup>15</sup>N) and 40 kHz (<sup>13</sup>C). During a contact time of 7 ms the <sup>1</sup>H radio frequency field was linearly varied about 20%.

UV/Vis optical diffuse reflectance spectra were collected at room temperature with a Varian Carry 500 UV/Vis diffuse reflectance spectrometer. Powders were prepared between two quartz discs at the edge of the integrating sphere with BaSO<sub>4</sub> as the optical standard. Absorption spectra were calculated from the reflectance data with the Kubelka-Munk function.

Argon sorption measurements were performed at 87 K with a Quantachrome Instrument Autosorb iQ. Samples of 20 mg were preheated in vacuum at 120 °C for 12 h. For BET calculations pressure ranges were chosen between 0.20-0.34 *p/p*<sub>0</sub>.

The pore size distribution was calculated from Ar adsorption isotherms by non-local density functional theory (NLDFT) using the “Ar-zeolite/silica cylindrical pores at 87 K” kernel (applicable pore diameters 3.5 Å – 1000 Å) for argon data as implemented in the AUTOSORB data reduction software.

Powder X-ray diffraction data were collected using a Bruker D8-advance diffractometer in reflectance Bragg-Brentano geometry employing Cu filtered CuK $\alpha$ -monochromator focused radiation (1.54059 Å) at 1600 W (40 kV, 40 mA) power and equipped with a Lynx Eye detector (fitted at 0.2 mm radiation entrance slit). Samples were mounted on Ge (111) sample holders after dispersing the powders with ethanol and letting the slurry dry to form a conformal film on the holder. The samples were measured with a 2 $\theta$ -scan from 2° to 30° as a continuous scan with 3046 steps and 5 s/step (acquisition time 4 h 47 min 45 s).

Transmission electron microscopy data were obtained with a Philips CM30/ST microscope with LaB<sub>6</sub> cathode, at an acceleration voltage of 300 kV. The powder was dispersed in *n*-Butanol. One drop of the suspension was placed on a holey carbon/copper grid.

Scanning electron microscopy images were obtained with a Zeiss Merlin at 1.5 kV. The TEM grids were deposited onto a sticky carbon surface.

## B. Synthetic Procedures

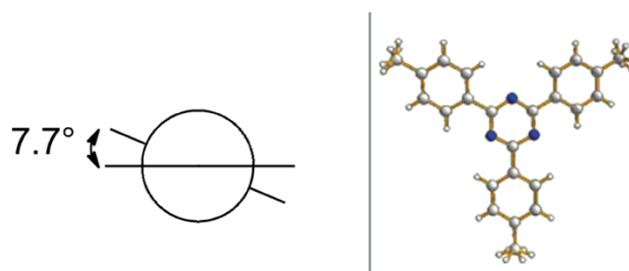
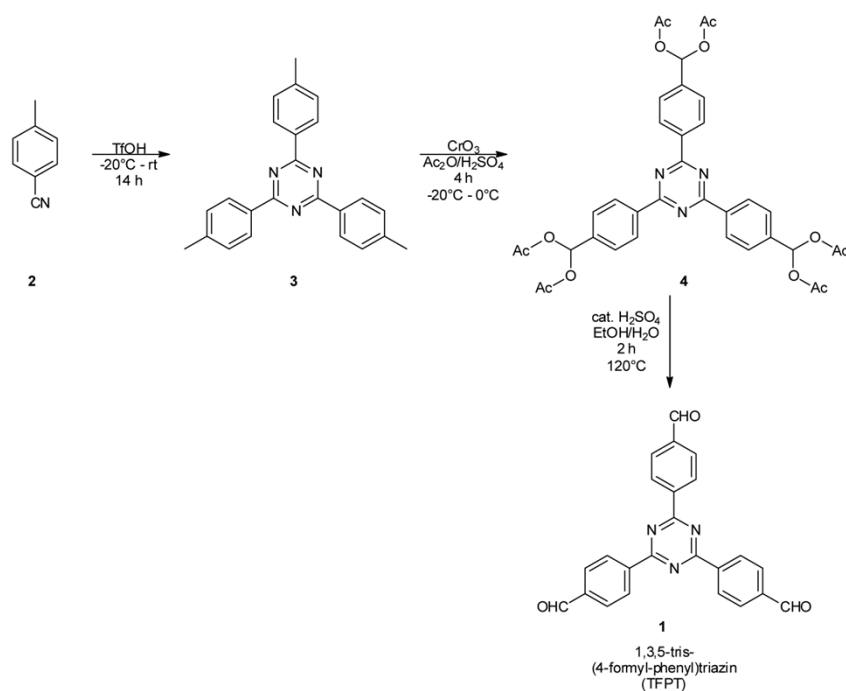
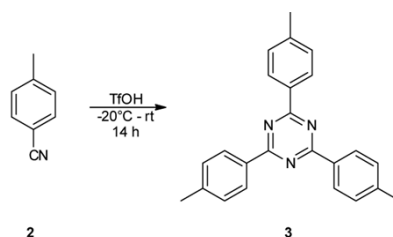


**Figure S1.** Molecular structure of 1,3,5-(4-methylphenyl)triazine. Newman projection on the single bond connecting triazine and phenyl ring (left) and structure derived from crystal data (right).<sup>S3</sup>



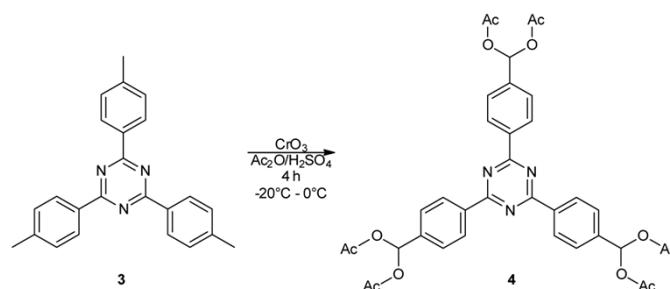
**Scheme S1.** Synthesis of 1,3,5-*tris*-(4-formyl-phenyl)triazine (TFPT) (**1**) by a three-step modified literature procedure.<sup>S2</sup>



**Scheme S2.** Synthesis of 1,3,5-*tris*-(4-methyl-phenyl)triazine (**3**) by super-acid catalyzed trimerization of *p*-tolunitrile (**2**) according to a literature procedure.<sup>S2</sup>

### 1,3,5-*tris*-(4-methyl-phenyl)triazine (**3**)

p-(**2**) (98%, Sigma Aldrich) was liquefied by putting the storage vessel in a 60 °C drying oven for 30 min. To a 25 ml round-bottom Schlenk flask with stir bar 5.0 ml (8.24 g, 53.8 mmol, 2.15 eq.) of triflic acid (AlfaAesar, 98%) were added and cooled to -20 °C in a dewar with salt/ice bath (1:3 v/v) under stirring. By syringe 3.1 mL (2.99 g, 25.0 mmol, 1.0 eq.) of **2** were added dropwise with help of a syringe pump over 1 h. The solution turned into a slurry solid over time and was left for 24 h. The cake was scratched off and transferred in ice water under stirring. This solution was neutralized with 4-5 mL 25% ammonia. The off-white precipitate was filtered off, washed with acetone (3 x 5 mL) and dried in vacuum to yield the title compound **3** (2.56 g, 7.29 mmol, 88%). <sup>13</sup>C and <sup>1</sup>H NMR data were consistent with the literature.

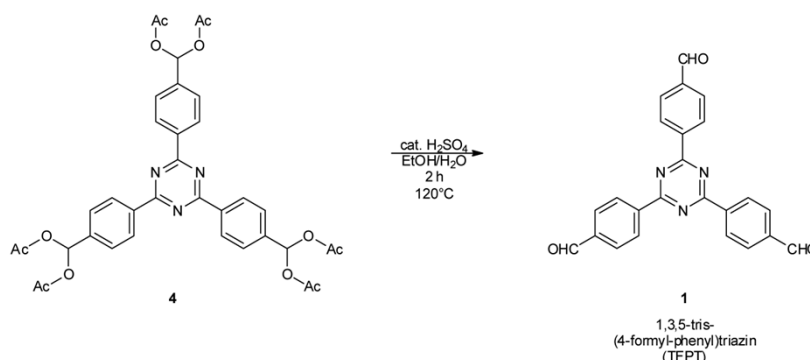


**Scheme S3.** Synthesis of [4,4',4''-(1,3,5-triazine-2,4,6-triyl)tris(4,1-phenylene)]-tris(methanetriyl)hexaacetate (**3**) by threefold benzylic oxidation of **3** by CrO<sub>3</sub> based on a modified literature procedure.<sup>S2</sup>

### [4,4',4''-(1,3,5-Triazine-2,4,6-triyl)tris(4,1-phenylene)]-tris(methanetriyl)hexaacetate (**4**)

To a 25 ml round-bottom flask with stir bar and rubber septum 100 mg (0.285 mmol, 1.0 eq.) of **3** and 1.00 mL of acetic anhydride were added and cooled down to -20 °C in a salt/ice bath. After addition of 0.2 ml 98% sulfuric acid, to the yellowish solution was added dropwise by syringe a solution of chromium(VI)oxide (250 mg, 92.6 mmol, 325 eq.) in 1.25 mL acetic anhydride over a period of 3.5 h under stirring. The temperature was kept below 0 °C. The greenish solution was stirred for another hour and then added dropwise to 12.5 mL stirred ice water. The yellowish precipitate was filtered off, washed with dest. water (3 x 3 mL) until neutral and dried in vacuum. The subsequent further purification by column chromatography (50:1 DCM/EtOAc) on silica gel yielded the title compound **4** (75 mg, 0.107 mmol, 38%).

<sup>13</sup>C and <sup>1</sup>H NMR data were consistent with the literature.



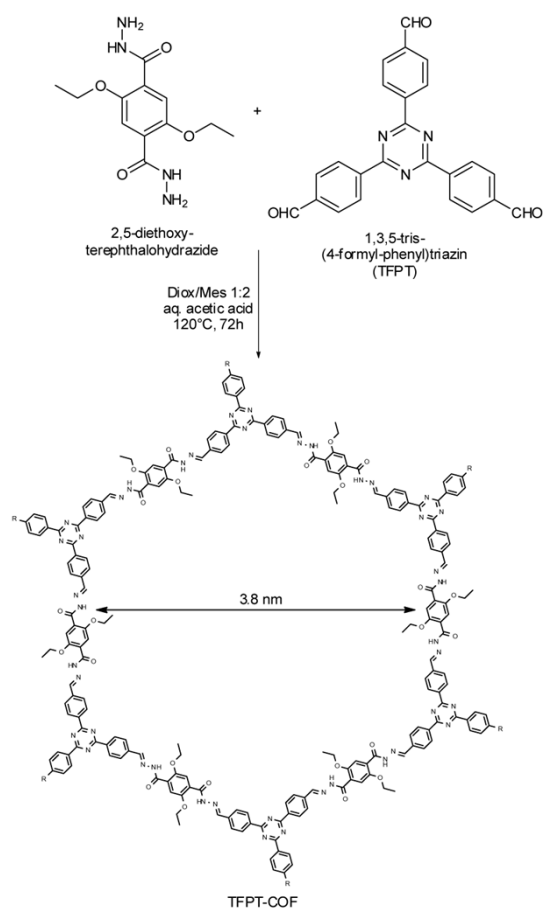
**Scheme S4.** Synthesis of 1,3,5-*tris*-(4-formyl-phenyl)triazine (TFPT) (**1**) by a microwave-assisted acid catalyzed deprotection based on a modified literature procedure.<sup>S2</sup>

### 1,3,5-*tris*-(4-formyl-phenyl)triazine (TFPT) (**1**)

To a stirred suspension of compound **4** (460 mg, 0.66 mmol, 1.0 eq) in 5.25 mL of dest. water and 4.20 mL of ethanol in a Biotage® 20 mL microwave vial was added 98% sulfuric acid (0.53 mL,

14.7 eq.). The vial was sealed and the resulting mixture was heated under microwave irradiation to 120 °C under stirring for 3 h. The resulting off-white precipitate was filtered, washed with water and dried under vacuum to yield title compound **1** (230 mg, 0.59 mmol, 89%).

<sup>1</sup>H NMR data were consistent with the literature.



**Scheme S5.** Synthesis of TFPT-COF by acid catalyzed hydrazone formation.

### TFPT-COF

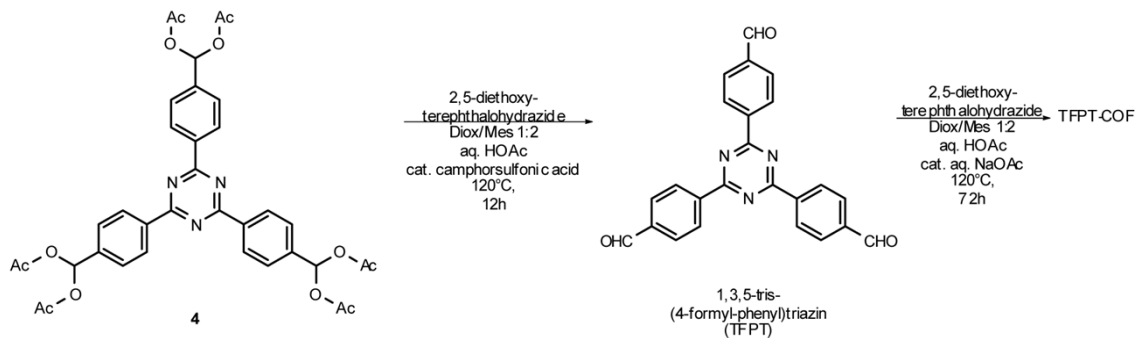
To a Biotage® 5 mL microwave vial 17.7 mg (0.044 mmol, 2.0 eq.) of TFPT (**1**) and a stir bar was added. Then 18.6 mg (0.066 mmol, 3.0 eq.) of 2,5-diethoxy-terephthalohydrazide was added and the vial was temporarily sealed with a rubber septum. Subsequently, the vial was flushed three times in argon/vacuum cycles. To the mixture 0.66 mL of mesitylene and 0.33 mL of 1,4-dioxane were added and again degassed three times in argon/vacuum cycles. In one shot 100  $\mu$ L aqueous 6M acetic acid was added, the vial was sealed and heated in a stirred oil bath with 120 °C (preheated) on a heating stirrer for 72 h. After slow cooling to room temperature the vial was opened and the whole mixture was centrifuged (3 x 15 min, 20000 rpm) while being washed with DMF (1 x 7 mL) and THF (2 x 7 mL). The resulting yellow precipitate was transferred to a storage vial with DCM, dried at room temperature, then in vacuum and characterized by powder X-ray diffraction.

Alternative workup: The vial was opened and the slurry suspension was transferred by a polyethylene pipette to a Büchner funnel and filtered. The filter cake was scratched off and transferred to an Erlenmeyer flask, washed with DMF (1 x 10 mL) and THF (2 x 10 mL) and again filtered off.

IR (FT, ATR): 3277 (w), 2966 (w), 2888 (w), 1674 (s), 1567 (m), 1515 (s), 1415 (m), 1356 (s), 1203 (vs), 1145 (m), 806 (s)  $\text{cm}^{-1}$ .

For elemental analysis the COF was wrapped in filter paper and then washed with THF in a microwave oven with THF (100 °C, 3 x 20 mL). Then the COF was activated in high-vacuum for 12 h at 120 °C at 10<sup>-7</sup> mbar and kept under an inert atmosphere until elemental analysis was performed.

Anal. Calcd. for  $(C_{84}H_{74}N_{18}O_{12})_n$ : C, 66.04; H, 4.88; N, 16.50. Found: C, 64.17; H, 4.96; N, 15.48.



**Scheme S6.** Synthesis of TFPT-COF by acid catalyzed in situ deprotection and subsequent hydrazone formation, carried out in one reaction vessel.

### TFPT-COF from protected TFPT ([4,4',4''-(1,3,5-Triazine-2,4,6-triyl)tris(4,1-phenylene)]-tris(methanetriyl)hexaacetate (4))

To a Biotage® 5 mL microwave vial 30.8 mg (0.044 mmol, 2.0 eq.) of **4** and a stir bar was added. Then 18.6 mg (0.066 mmol, 3.0 eq.) of 2,5-diethoxy-terephthalohydrazide was added and the vial was temporarily sealed with a rubber septum. Subsequently, the vial was flushed three times in argon/vacuum cycles. To the mixture 0.66 mL of mesitylene and 0.23 mL of 1,4-dioxane were added and again degassed three times in argon/vacuum cycles. In one shot 100  $\mu$ L aqueous 6M acetic acid was added. To this vial, 0.10 mL ( $c = 20 \text{ mg mL}^{-1}$ , 0.008 mmol, 0.38 eq.) of a solution of *rac*-camphorsulfonic acid in 1,4-dioxane was added, the vial was sealed and heated in a stirred oil bath with 120 °C (preheated) on a heating stirrer for 12 h. After cooling to room temperature, to the vial was added 0.02 mL ( $c = 35 \text{ mg mL}^{-1}$ , 0.008 mmol, 0.38 eq.) of an aqueous solution of sodium acetate by a micro syringe. The vial was then reheated again on the preheated oil bath for 72 h at 120 °C. After slow cooling to room temperature the vial was opened and the whole mixture was centrifuged (3 x 15 min, 20000 rpm) while being washed with DMF (1 x 7 mL) and THF (2 x 7 mL). The resulting yellow precipitate was transferred to a storage vial with DCM, dried at room temperature, then in vacuum and characterized by powder X-ray diffraction.

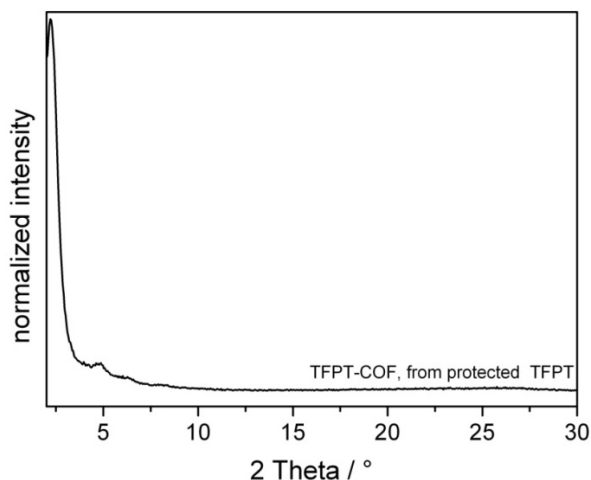


**Figure S2.** PXRD of the TFPT-COF from protected TFPT.

### TFPT-COF reconverted after sonication in water/photocatalysis

To a Biotage® 5 mL microwave vial 20 mg of amorphous TFPT-COF and a stir bar were added. The vial was temporarily sealed with a rubber septum. Subsequently, the vial was flushed three times in argon/vacuum cycles. To the mixture 0.66 mL of mesitylene and 0.33 mL of 1,4-dioxane were added and again degassed three times in argon/vacuum cycles. In one shot 100  $\mu$ L aqueous 6M acetic acid was added. The vial was sealed and heated in a stirred oil bath with 120 °C (preheated) on a heating stirrer for 72 h. After slow cooling to room temperature the vial was opened and the whole mixture was centrifuged (3 x 15 min, 20000 rpm) while being washed with DMF (1 x 7 mL) and THF (2 x 7 mL). The resulting yellow precipitate was transferred to a storage vial with DCM, dried at room temperature, then in vacuum and characterized by powder X-ray diffraction and BET surface area determination.

### C. FT-IR Spectra

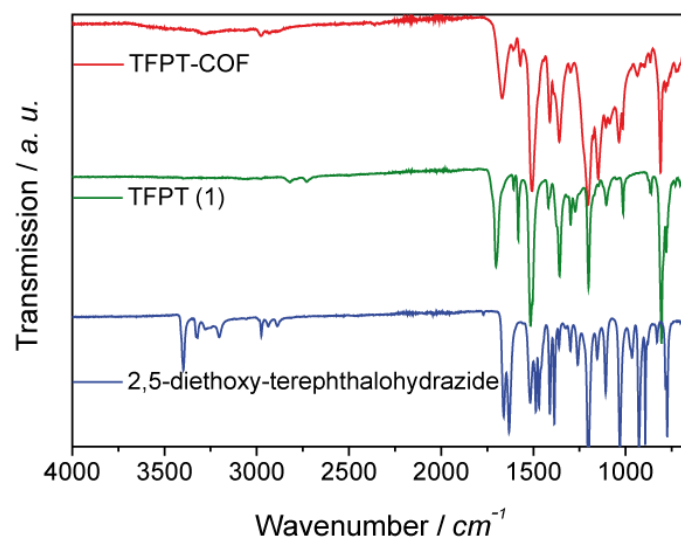


Figure S3. Stack plot FT-IR spectra of TFPT-COF and starting materials.

Table S1. IR assignments for TFPT (green), DETH (blue) and TFPT-COF (red).

Wavenumber [ $\text{cm}^{-1}$ ]	Band Assignment
2824, 2721	Fermi double peak, aldehyde C-H (specific)
>3200	N-H stretching
1700	Aldehyde C=O stretching
1632, 1660, 1670-1660, 1201	C=O stretching, C=N
806, 806	triazine ring breath

## D. CP-MAS NMR Measurements

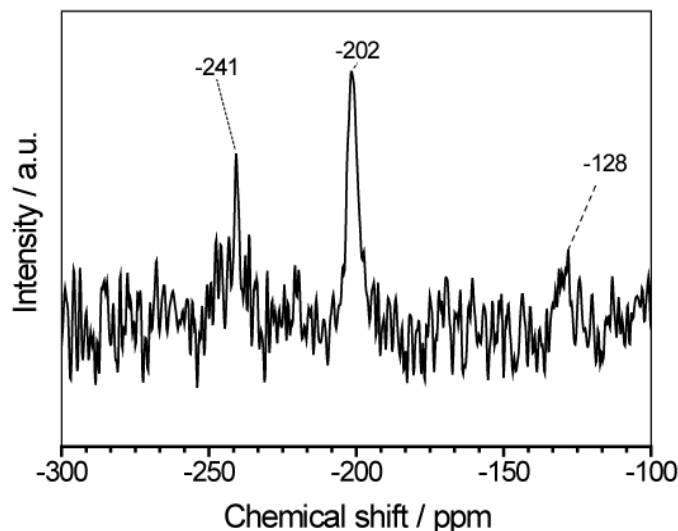


Figure S4. <sup>15</sup>N CP-MAS spectrum of TFTP-COF.

The <sup>15</sup>N CP-MAS NMR spectrum exhibits a peak at -241 ppm, which we assign to the tertiary nitrogen of the hydrazone moiety, the peak at -202 ppm to the hydrazine secondary nitrogen, and the peak at -128 ppm to the nitrogen of the triazine ring.

## E. Powder X-Ray Diffraction Data and Structure Simulation

Molecular modeling of the COF was carried out using the Materials Studio (5.5) suite of programs by Accelrys.

The unit cell was defined by two TFPT molecules bonded via six hydrazone linkages to 2,5-diethoxyterephthalohydrazide. The initial structure was geometry optimized using the MS Forcite molecular dynamics module (Universal force fields, Ewald summations), and the resultant distance between opposite formyl carbon atoms in the structure was used as the *a* and *b* lattice parameters (initially 43 Å) of the hexagonal unit cell with *P6/m* symmetry (*bnn* net). The interlayer spacing *c* was chosen as 3.37 Å according to the 001 stacking reflection of the powder at  $2\theta = 26.6^\circ$ , and the crystal structure was geometry optimized using Forcite (resulting in  $a = b = 43.164$  Å).

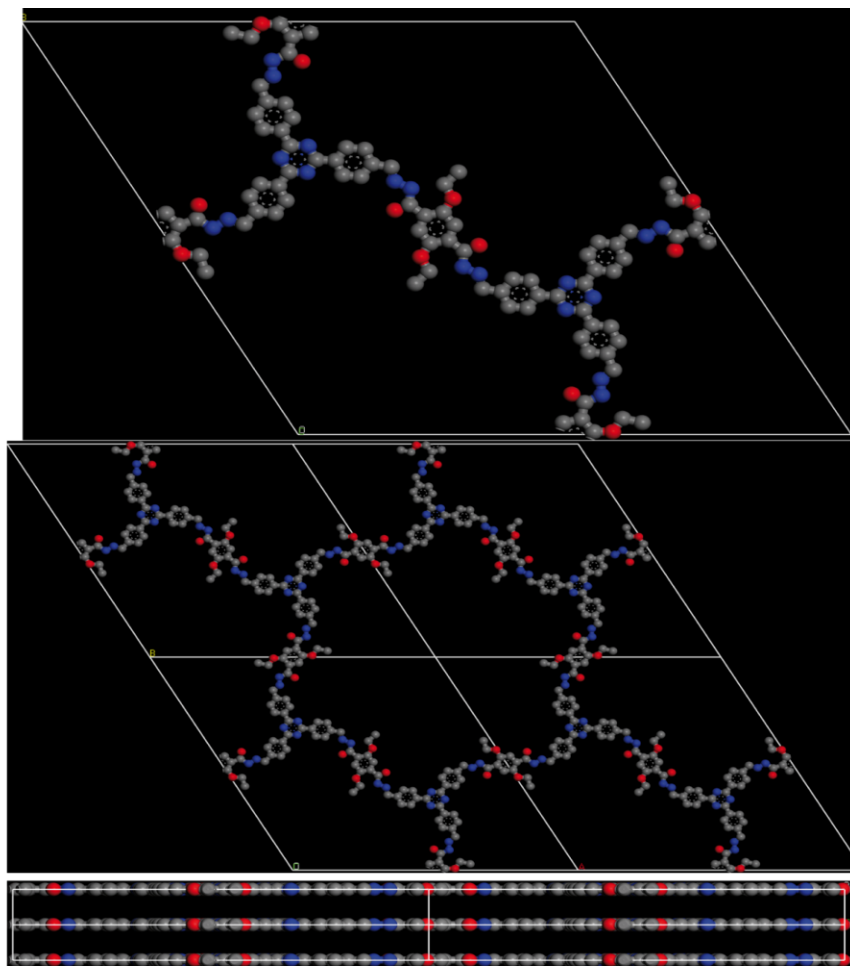


**Figure S5.** Simulation of the unit cell content calculated in an eclipsed arrangement: top view onto the *ab*-plane and view perpendicular to the *c*-axis.

The MS Reflex Plus module was then used to calculate the PXRD pattern, which matched the experimentally observed pattern closely in both the positions and intensity of the reflections. The observed diffraction pattern was subjected to Pawley refinement wherein reflection profile and line shape parameters were refined using the crystallite size broadening (one size was extracted from the exp. PXRD with the help of the Scherrer equation  $\rightarrow$  crystal size:  $c = 35$  nm, kept fixed) and background in the 20<sup>th</sup> polynomial order.

The refinement was applied to the calculated lattice, producing the refined PXRD profile with lattice parameters  $a = b = 41.895$  Å and  $c = 3.37$  Å.  $wRp$  and  $Rp$  values converged to 3.30% and 6.73%, respectively. The resulting refined crystallite size (149 nm in each lateral direction) is in reasonable agreement with the SEM and TEM data. Overlay of the observed and refined profiles shows good correlation (Figure S6).

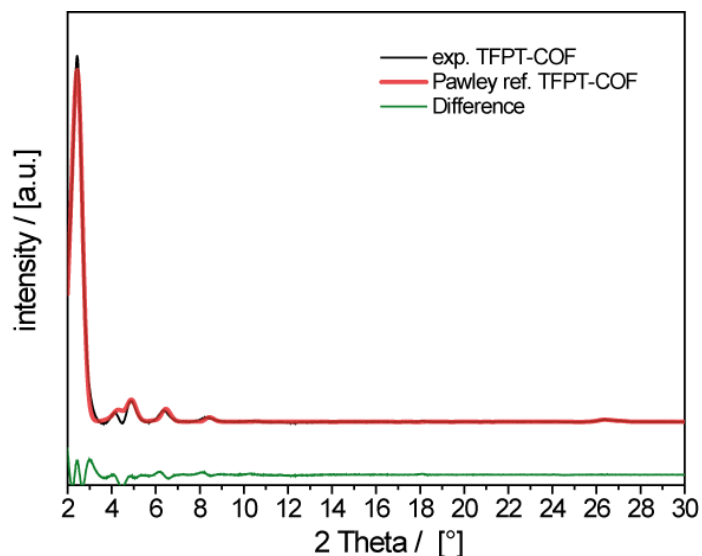


**Figure S6.** Experimental powder pattern and Pawley refined pattern based on  $P6/m$  symmetry.

**Table S2.** Atom coordinates of optimized  $P6/m$  structure.

Atomic parameters					
Atom	Ox.	Wyck.	x/a	y/b	z/c
C1		6j	4.46484	0.49326	0
C2		6j	4.46961	0.46288	0
C3		6j	4.50666	0.46983	0
C7		6j	4.47874	0.55594	0
O8		6j	4.56434	0.57050	0
C10		6j	4.43337	0.39480	0
C11		6j	4.39330	0.36475	0
O14		6j	4.44518	0.54253	0
N15		6j	4.50051	0.59501	0
N19		6j	4.52013	0.38747	0
C21		6j	4.49094	0.64722	0
C23		6j	4.53965	0.34528	0
C25		6j	4.46512	0.69023	0
C26		6j	4.43386	0.69438	0
C27		6j	4.39837	0.66301	0
C28		6j	4.39415	0.62805	0
C29		6j	4.42460	0.62405	0
C30		6j	4.36484	0.66515	0
N31		6j	4.36636	0.69806	0

Even lower  $wRp$  and  $Rp$  values (1.94% and 3.94%) could be achieved by lowering the symmetry to  $P1$  (Figure S7) but keeping the angles  $\alpha$ ,  $\beta$  and  $\gamma = 90^\circ$ ,  $90^\circ$  and  $120^\circ$ . The resulting lattice parameters  $a$  and  $b$  were = 42.055 Å and 45.074 Å.

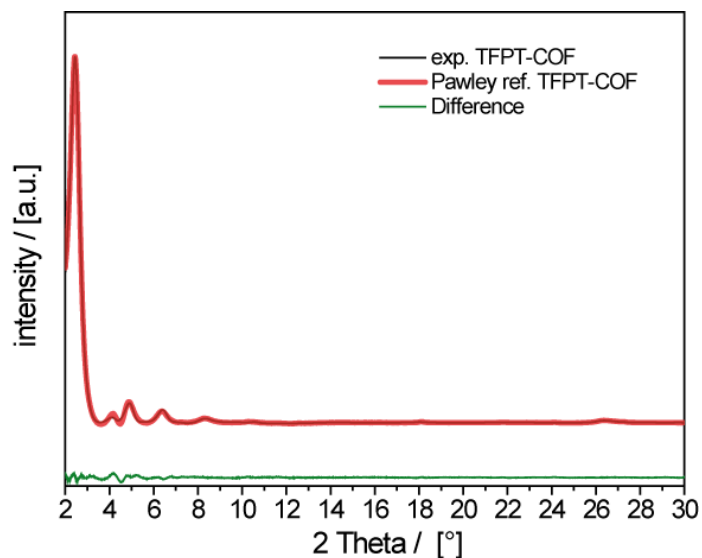


**Figure S7.** Experimental powder pattern and Pawley refined pattern based on  $P1$  symmetry.

An alternative staggered COF arrangement was examined wherein  $P63/m$  symmetry was used (*gra* net). Comparison of the calculated PXRD pattern with the observed pattern shows less agreement with the experimental data (see Fig. 2), thus ruling out this type of packing arrangement.

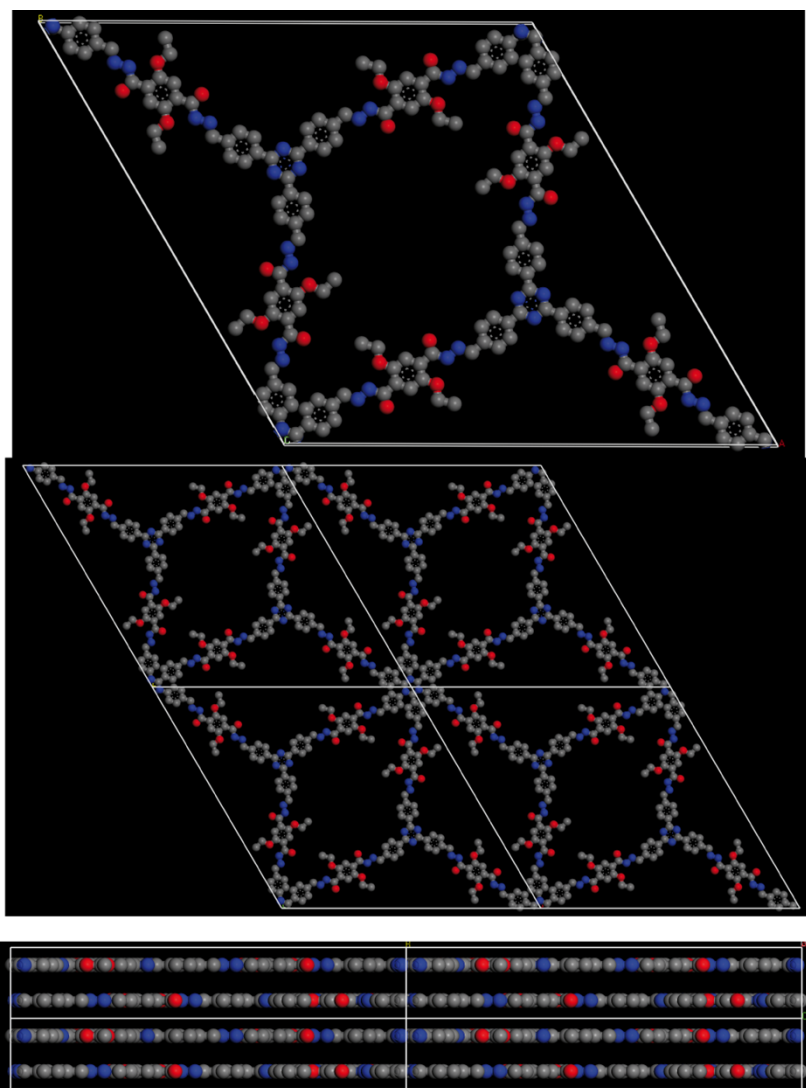


**Figure S8.** Simulation of the crystal structure with staggered arrangement of adjacent layers: Top view onto the  $ab$ -plane and view perpendicular to the  $c$ -axis showing the doubled stacking period due to the staggered AB layer arrangement.

In a recent theoretical study on boronate COFs, Dichtel *et al.* (ref. 42) and Heine (ref. 41) pointed out that two adjacent layers in a COF are not expected to be aligned in a perfectly eclipsed manner, but shifted between  $\approx 1.3 - 1.8 \text{ \AA}$  in any direction parallel to the layer (parallel displacement).

We therefore simulated (using the software package Material Studio) an AA'A-structure of TFPT-COF where adjacent layers are offset by  $1.4 \text{ \AA}$ , such that each partly positively charged carbon atom of triazine is situated beneath a partly negatively charged triazine nitrogen atom, which was found to be a likely structure for triazine units. The structure was simulated in *P1* symmetry with lattice parameters  $a = b = 42.16 \text{ \AA}$  and  $c = 6.74 \text{ \AA}$  ( $c$  axis doubled due to symmetry reasons).

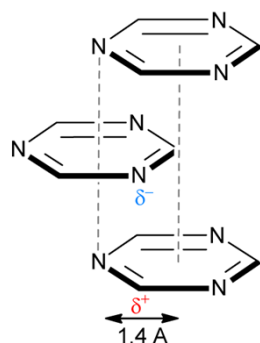


**Figure S9.** Shift (parallel displacement) in a zig-zag manner to minimize electrostatic repulsion between adjacent layers.

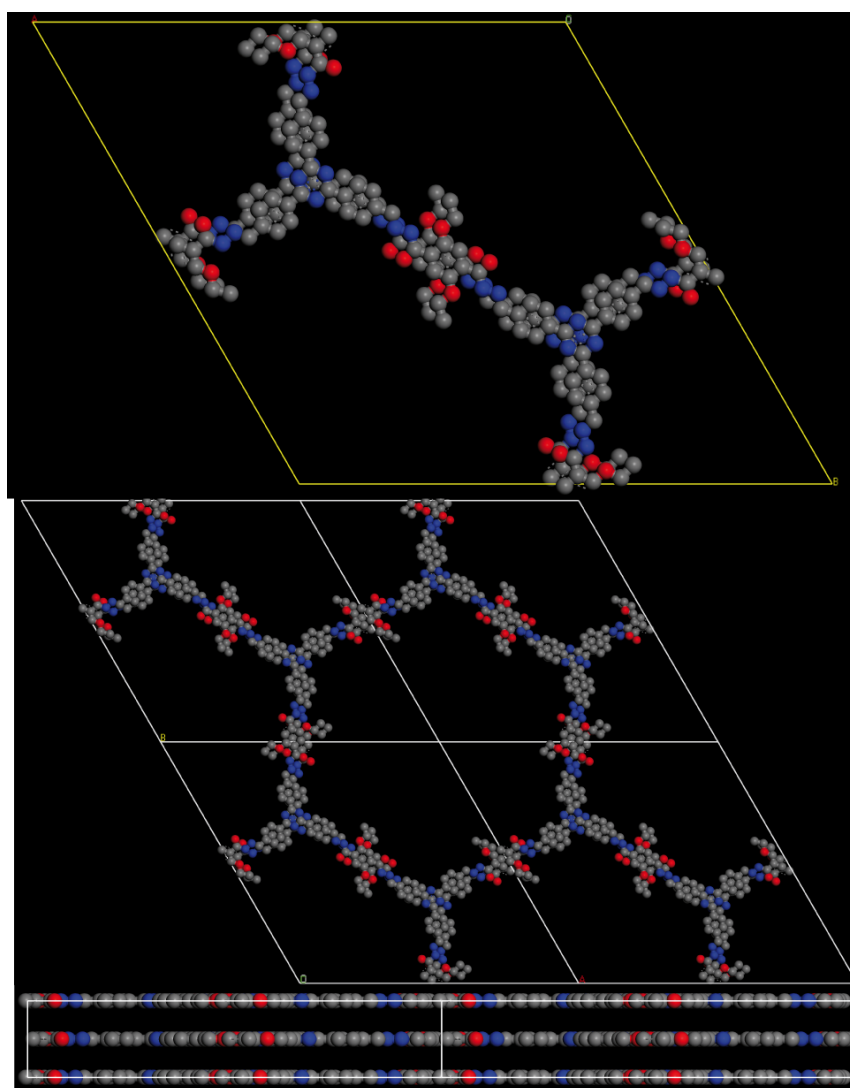


**Figure S10.** Simulation of the unit cell content calculated in an eclipsed arrangement with  $1.4 \text{ \AA}$  offset and zig-zag-arrangement of the layers: View onto the  $ab$ -plane (top) and view perpendicular to the  $c$ -axis (bottom).

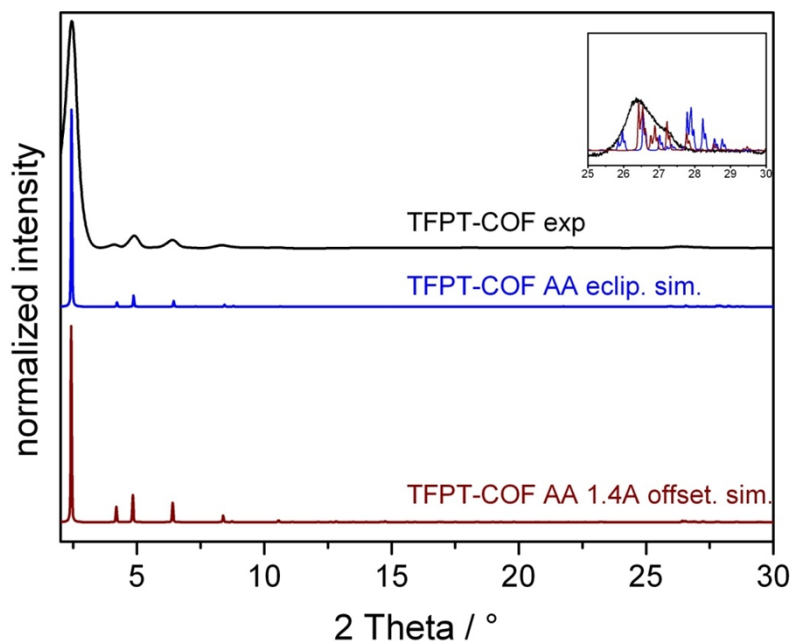


**Figure S11.** Experimental powder pattern (black), simulated PXRD of perfectly eclipsed TFPT-COF (blue) and simulated PXRD of TFPT-COF with 1.4 Å parallel layer displacement (red).

## F. Sorption Measurements and Pore Size Distribution

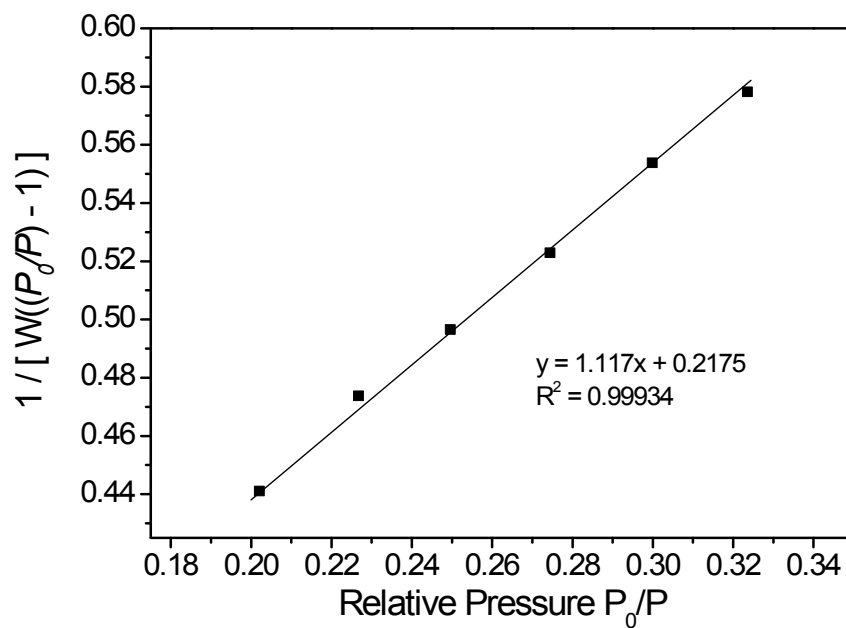


**Figure S12.** Linear BET plot of TFPT-COF as obtained from Ar adsorption data at 87 K.

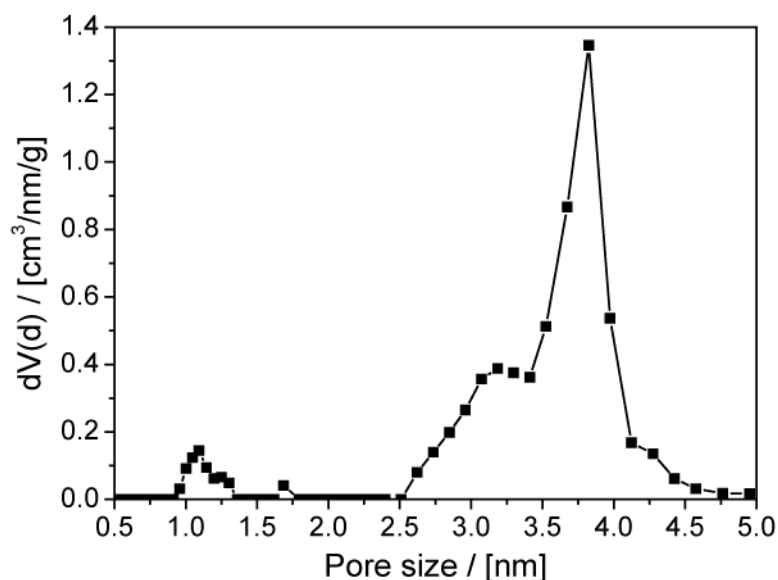


**Figure S13.** Pore size distribution calculated based on NLDFT using the “Ar-zeolite/silica cylindrical pores at 87 K kernel.

The Brunauer-Emmett-Teller (BET) surface area was calculated to be  $1603 \text{ m}^2 \text{ g}^{-1}$  (linear extrapolation between 0.20-0.32  $p/p_0$ ).

### G. Plot of the Kubelka-Munk Function

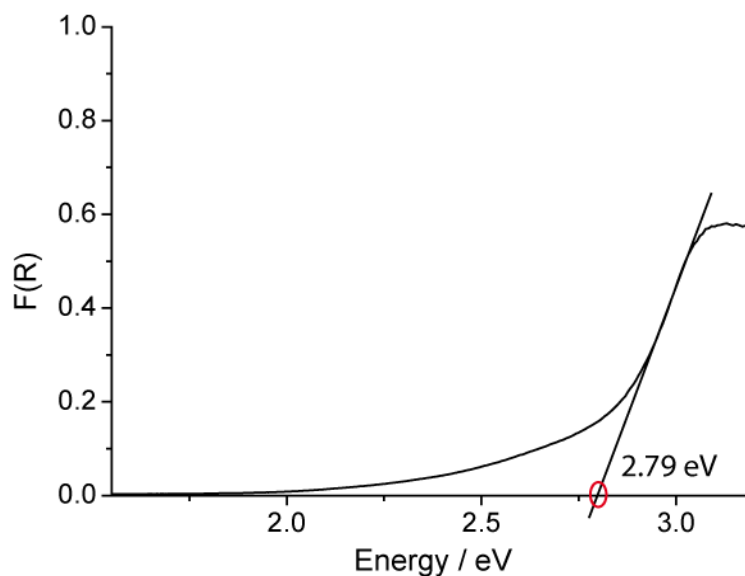


**Figure S14.** Plot of Kubelka-Munk function used for band gap extraction.

### H. Stability of TFPT-COF in Organic Solvents and Water

Stability in different organic solvents (DCM, DMF and MeOH) has been tested by soaking TFPT-COF (5 mg) in the corresponding solvent for 3 h at room temperature. A PXRD was recorded after filtration and drying in vacuum overnight.

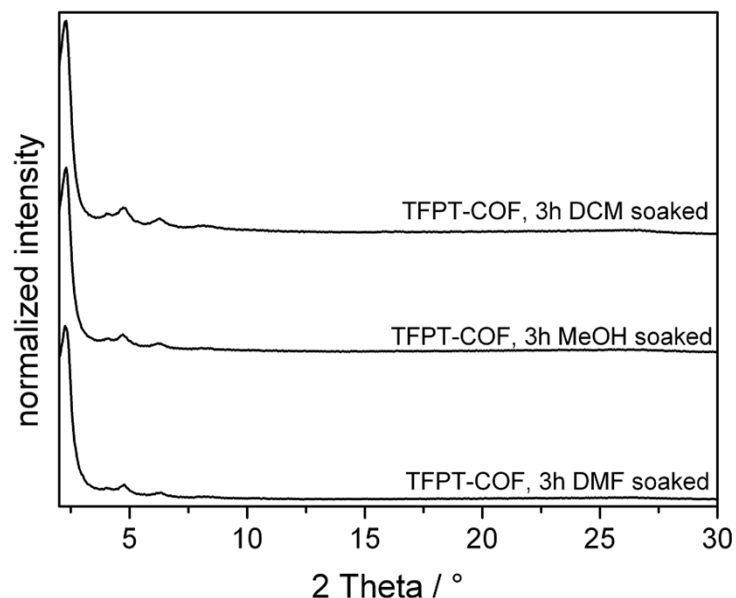


**Figure S15.** PXRD measurements showing the retention of crystallinity after treatment with different solvents.

### I. Reconversion of TFPT-COF after photocatalysis

20 mg of crystalline TFPT-COF (BET surface area =  $1190 \text{ m}^2\text{g}^{-1}$ ) was used for photocatalytic hydrogen production as described below. After irradiation with visible light for 95 h the TFPT-COF/Pt was filtered off as a green and amorphous solid (Fig. S21) and washed with water, DMF (2 x 7 mL) and THF (2 x 7 mL). The organic filtrates were checked for any formed monomers (e.g. TFPT or DETH), but no traces of monomeric species were detected. The TFPT-COF/Pt has lost its crystallinity after photocatalysis as shown in Fig. S16, and has a BET surface area of  $410 \text{ m}^2\text{g}^{-1}$  (Fig. S18). The vacuum-dried powder can be reconverted (see section B) to recover crystalline TFPT-COF with its original PXRD pattern (Fig S.16) and a high BET surface area of  $1184 \text{ m}^2\text{g}^{-1}$  (Fig. S18) (yield: 14 mg, 70%) by resubjecting it to the initial synthesis conditions. An Ar sorption isotherm of TFPT-COF/Pt<sub>reconv.</sub> was recorded and is shown in Fig. S19. The corresponding pore size distribution is depicted in Fig. S20, having a maximum at 3.7 nm. Further experiments revealed that the TFPT-COF has already lost its long-range order after sonication in water (Fig. S16). However, the FTIR spectrum shows the characteristic bands of the polymer (C=N at  $1603 \text{ cm}^{-2}$ ), while no additional peaks appear and no bands corresponding to the TFPT or DETH monomers are observed (Fig. S17). The vacuum-dried powder can also be reconverted (see section B) to recover TFPT-COF with its original PXRD pattern (Fig S.16).

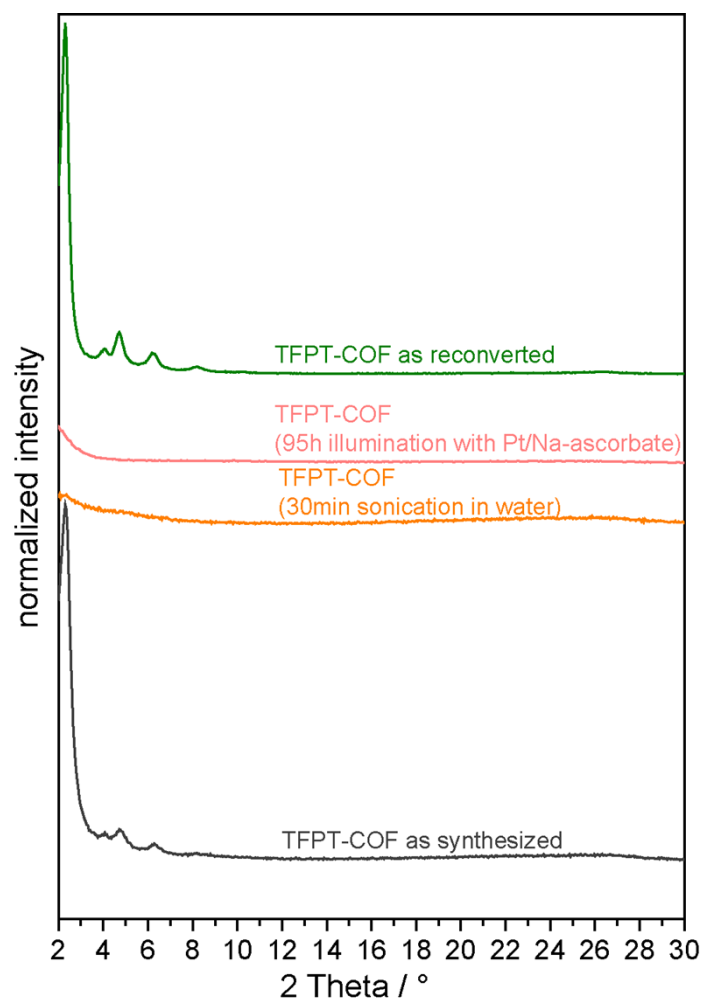


**Figure S16.** PXRD patterns of TFPT-COF, showing loss of crystallinity after water exposure and photocatalysis. The crystalline TFPT-COF can be obtained by reversion by subjecting it to the initial crystallization conditions.

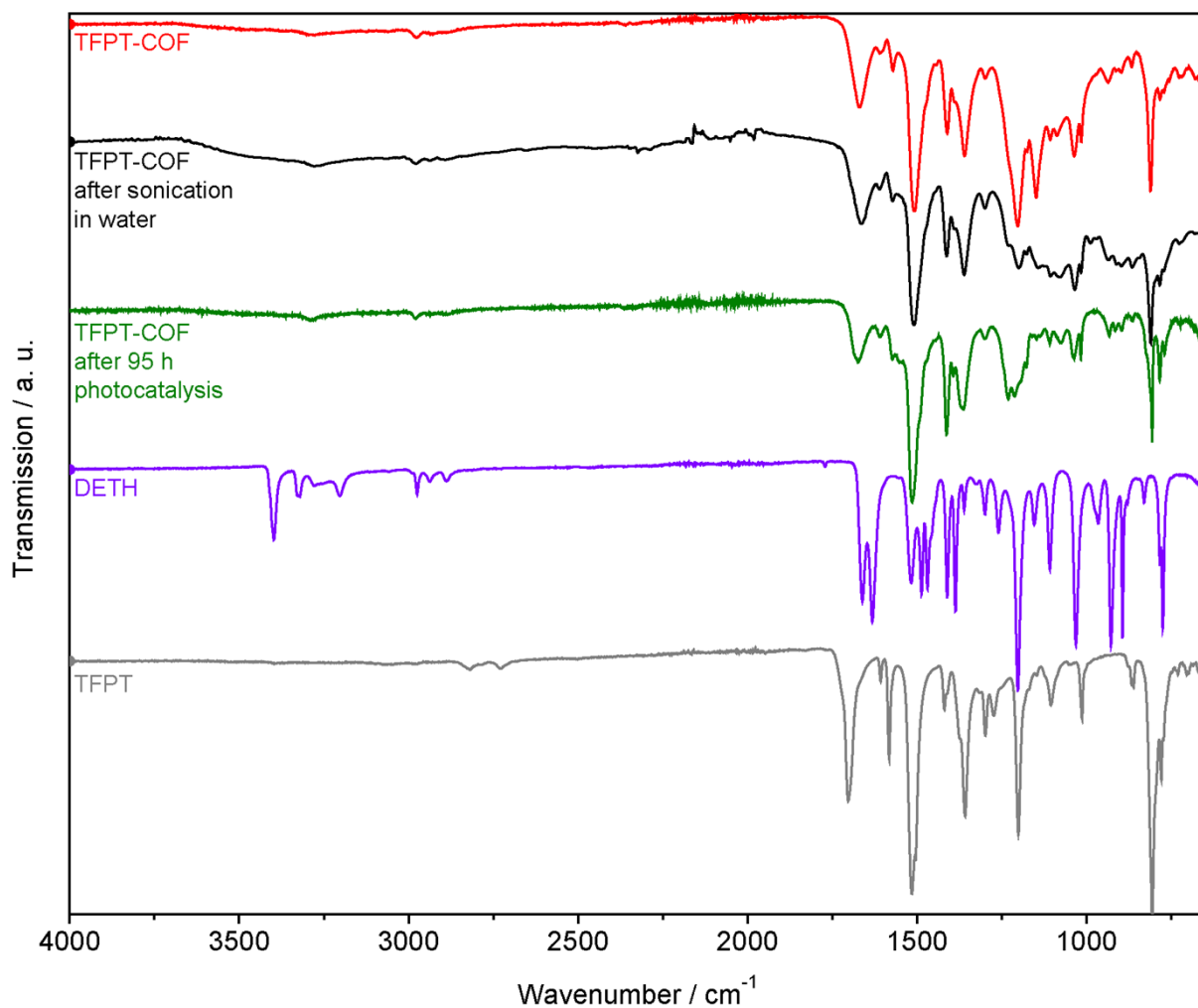


**Figure S17.** FT-IR spectra showing the vibrational patterns of TFPT-COF before and after water exposure/photocatalysis.

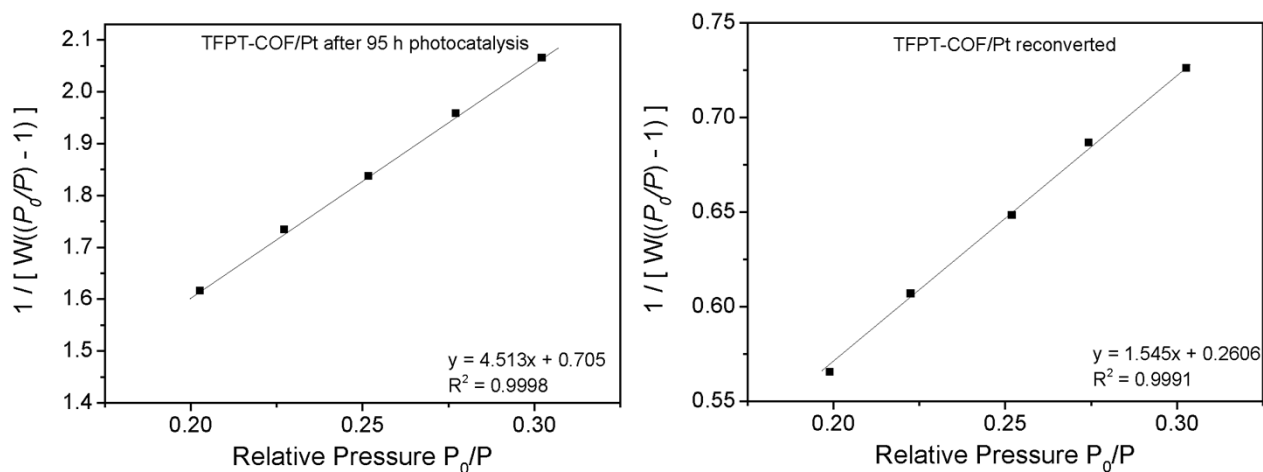


**Figure S18.** Linear BET plot of TFPT-COF/Pt after 95 h photocatalysis and TFPT-COF/Pt (reconverted) as obtained from Ar adsorption data at 87 K.

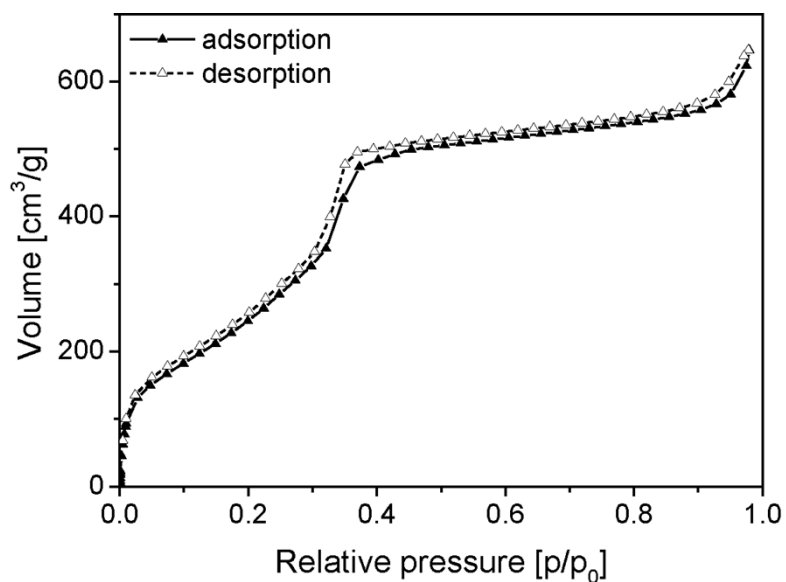


**Figure S19.** Ar sorption isotherm recorded at 87 K.

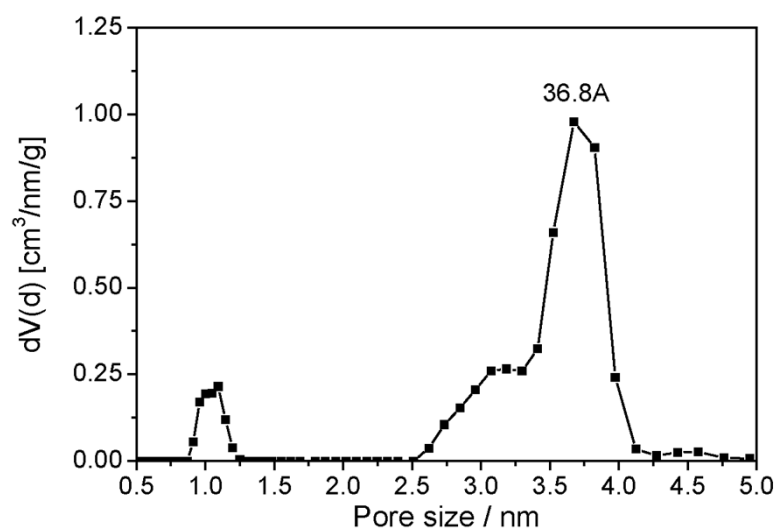


**Figure S20.** Pore size distribution of TFPT/Pt after reconversion calculated based on NLDFT using the “Ar-zeolite/silica cylindrical pores at 87 K” kernel.



**Figure S21.** Photographs showing TFPT-COF as-synthesized (left, yellow) and TFPT-COF/Pt after reconversion (right, green). TFPT-COF/Pt before reconversion is green, as well.

## J. Photocatalysis

For long-time hydrogen evolution experiments in triethanolamine, the TFPT-COF catalyst (4 mg) was suspended in water (9 mL) and dispersed in an ultrasonic bath for 30 min. The sacrificial electron donor (1 mL) triethanolamine (TEoA, Alfa Aesar) and  $\text{H}_2\text{PtCl}_6$  (2.4  $\mu\text{L}$  of 8 wt% in  $\text{H}_2\text{O}$ , Sigma-Aldrich,  $\approx 2.2$  wt% Pt) as precursor for the in situ formation of the Pt cocatalyst was added. For long-time hydrogen evolution experiments in sodium ascorbate, the TFPT-COF catalyst (10 mg) was suspended in water (10 mL) and dispersed in an ultrasonic bath for 30 min. Sodium ascorbate as sacrificial electron donor (100 mg) (Sigma-Aldrich,  $\geq 98\%$ ) and  $\text{H}_2\text{PtCl}_6$  (6.0  $\mu\text{L}$  of 8 wt% in  $\text{H}_2\text{O}$ , Sigma-Aldrich,  $\approx 2.2$  wt% Pt) was added. The induction time and concomitant delay in hydrogen evolution observed in the first cycle is caused by the initial formation of Pt nanoparticles (induction time). The first cycle represents the first three hours of the long-term measurement – the induction time period – where Pt nanoparticles are formed by the photoreduction of  $\text{H}_2\text{PtCl}_6$ . For each cycle the photocatalyst (Pt-doped COF) was separated from its suspension (for the photocatalytic measurements) by centrifugation and was washed several times with water. The dried photocatalyst was redispersed with a fresh sodium ascorbate solution (10 mL of water and 100 mg of sodium ascorbate) and illuminated for 3 hours ( $< 420$  nm) for each cycle.

For visible light and UV experiments the suspensions were illuminated at a distance of 26 cm from the light source in a 230 mL quartz glass reactor with a PTFE septum under argon atmosphere. The flask was evacuated and purged with argon to remove any dissolved gases in the solution. Samples were simultaneously top-illuminated (top surface = 15.5  $\text{cm}^2$ ) with a 300 W Xenon lamp with a water filter and dichroic mirror blocking wavelengths  $< 420$  nm for visible light measurements while stirring. For wavelength-specific measurements, the full spectrum of the Xenon lamp coupled with a band-pass filter (400, 450, 500, 550 or 600 nm; bandwidth  $\pm 20$  nm) and an 1.5 AM filter was used. Here, an aqueous triethanolamine suspension with 10 mg of Pt-doped catalyst was illuminated for three hours and the concentration of evolved hydrogen was determined by gas chromatography. The intensity of the light was measured for each wavelength, enabling the conversion of produced hydrogen values into quantum efficiencies. For oxygen evolution measurements photodeposition of  $\text{IrO}_2$  nanoparticles as oxygen-evolving cocatalyst was carried out before the photocatalytic reaction following a literature procedure.<sup>S4,5</sup> To this end, 40 mg of the catalyst was dispersed in a reactant solution containing  $\text{K}_2[\text{IrCl}_6]$  (1.8 mg,  $\approx 2$  wt%, Alfa Aesar) and 40 mL of a 5 mM aqueous  $\text{KNO}_3$  solution. The suspension was irradiated as described above for 2 h using the full spectrum of the Xenon lamp. The TFPT-COF catalyst loaded with the cocatalyst was isolated from the aqueous  $\text{KNO}_3$  solution, washed several times with water, and then dried at 100  $^\circ\text{C}$  in a stream of argon. The  $\text{IrO}_2$ -loaded catalyst (10 mg) was dispersed in phosphate buffer solution (10 mL, 0.1 M, pH = 11 or pH = 7).  $\text{Na}_2\text{S}_2\text{O}_8$  (110 mg, Sigma-Aldrich) or  $\text{AgNO}_3$  (16 mg) was added as electron acceptor. The headspace of the reactor was periodically sampled with an online injection system and the gas components were quantified by gas chromatography (thermal conductivity detector, argon as carrier gas).

The quantum efficiency of the photocatalysts, under irradiation with the band-pass filter  $500 \pm 20$  nm, was determined as follows. The power of the incident light was measured with a thermo power sensor (Thorlabs) to be 14  $\text{mW cm}^{-2}$ , which is equivalent to a photon flux of 701  $\mu\text{mol h}^{-1}$ . Quantum efficiency was calculated using the equation:

$$\text{QE} = 2 \cdot [\text{H}_2] / I$$

where  $I$  is the photon flux in  $\mu\text{mol h}^{-1}$  and  $[\text{H}_2]$  is the average rate of  $\text{H}_2$  evolution in  $\mu\text{mol h}^{-1}$ .

## K. Stability of TFPT-COF during photocatalysis

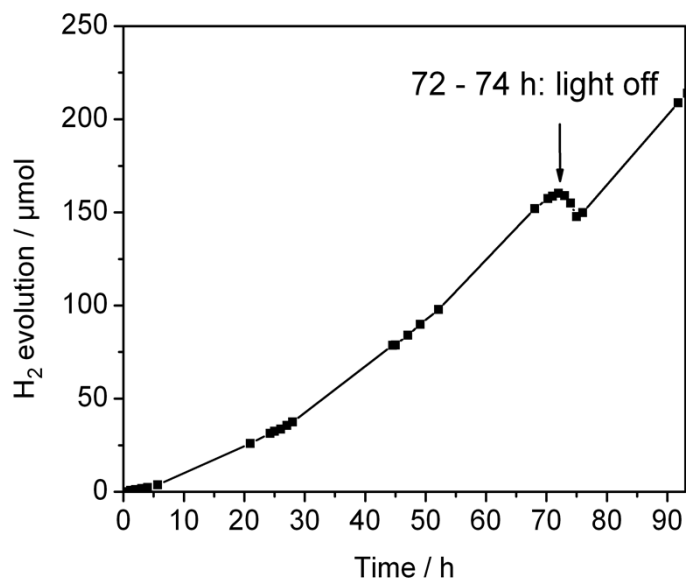


**Figure S22.** Stability measurements of TFPT-COF for 95 h with ascorbate as sacrificial donor. Between the 72<sup>th</sup> and 74<sup>th</sup> hour the light source was turned off to show no hydrogen evolution in the dark (the amount of hydrogen concentration decreased during these hours due to the fact that sampling was performed, i.e. removing sample volume during detection).

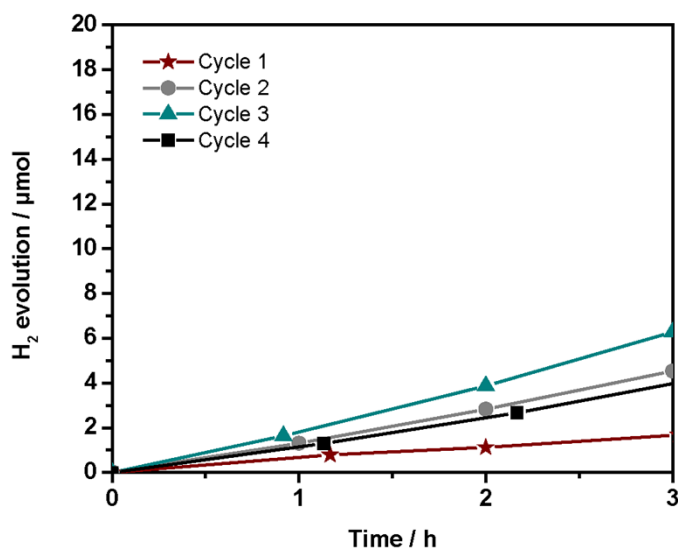


**Figure S23.** Cycle measurements of TFPT-COF/Pt with sodium ascorbate as sacrificial donor. The first cycle (Cycle 1) corresponds to the first three hours of the long-term stability measurements (95 h) and shows decreased rates due to formation of Pt nanoparticles (induction period). The other cycles were carried out after centrifugation of the photocatalyst, washing with water and resuspending it in a fresh aqueous sodium ascorbate solution.

## L. References

- S1 Uribe-Romo, F. J.; Doonan, C. J.; Furukawa, H.; Oisaki, K.; Yaghi, O. M. *J. Am. Chem. Soc.* **2011**, *133*, 11478–11481.
- S2 Li, S.-H.; Huang, H.-P.; Yu, S.-Y.; Li, X.-P. *Chin. J. Chem.* **2006**, *24*, 1225–1229.
- S3 Volkis, V.; Nelkenbaum, E.; Lisovskii, A.; Hasson, G.; Semiat, R.; Kapon, M.; Botoshansky, M.; Eishen, Y.; Eisen, M. S. *J. Am. Chem. Soc.* **2003**, *125*, 2179–2194.
- S4 Ikeda, T.; Tsuda, A.; Aratani, N.; Osuka, A. *Chem. Lett.* **2006**, *35*, 946–947.
- S5 Sabio, E. M.; Chamousis, R. L.; Browning, N. D.; Osterloh, F. E. *J. Phys. Chem. C* **2012**, *116*, 3161–3170.